

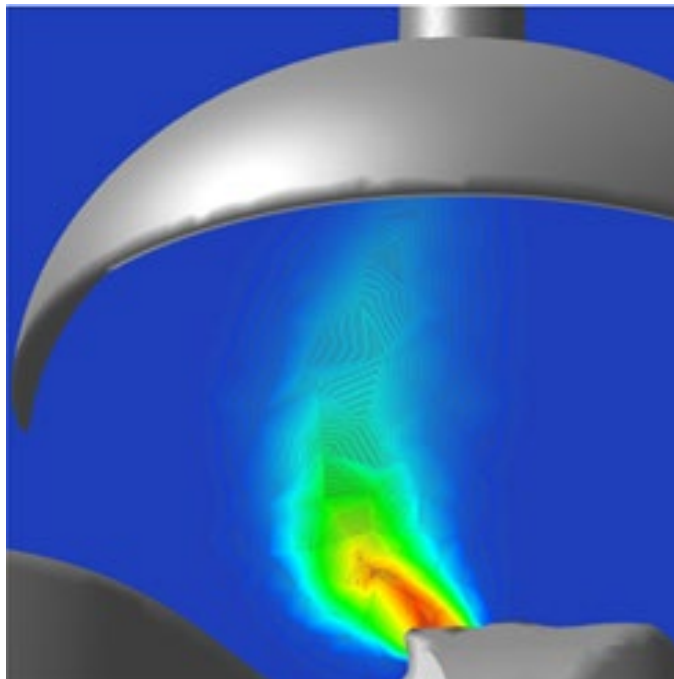
Tracking and Controlling the Airborne Spread of the Flows Originated from Aerosol Generating Dental Procedures – a Multiphase Flows Study on Covid-19 Airborne Transmission

Mojtaba Zabihi¹, Stephen Munro², Jonathan Little³, Sunny Li¹, Joshua Brinkerhoff¹, Sina Kheirkhah¹

¹: School of Engineering, Faculty of Applied Science, UBC

²: CareHealth Meditech

³: School of Health and Exercise Sciences, Faculty of Health and Social Development, UBC



October 2020



THE UNIVERSITY OF BRITISH COLUMBIA



Abstract

Since its emergence in December 2019, SARS-COV2 and the resultant Corona Virus Disease 2019 (COVID-19) has impacted almost all countries, affecting more than 44 million patients and creating a global public health threat [1]. The routes of transmission are direct contact, droplet, and aerosol transmissions. Many dental procedures are considered Aerosol Generating Procedures (AGPs). Despite of using standard control measures (e.g. high volume evacuation, rubber dams), these AGPs emit uncontrolled aerosols and droplets, which are referred to as AGP flows. Controlling and eliminating the AGP flows are important components for controlling infection risk for both patients and oral health care providers. A multiphase flows computational fluid dynamics (CFD) simulation was conducted to track the flow of aerosols and droplets in a room during dental AGPs. Two numerical models were considered. The first model is a dental office without any extra control of AGP flows during the dental procedure. The results showed droplets and aerosols are expected to spread widely, over a relatively long period of time inside the dental office. For this case, fallow time needs to be taken as the mitigation technique, which relies on the HVAC system to change the room air. The second model is a dental office installed with a portable extra oral suction device, for which the AIIR device by Care Health Meditech Developments Inc. was used as an example. The results showed such device provides *local* and *synchronous* control of AGP flows, with the device quickly isolating and eliminating the AGP flows from spreading and travelling in the dental operatory.

1. Introduction

Aerosol Generating Procedures (AGPs) refer to medical procedures that result in significant production of liquid particles with a wide range of size. Particles with sub-micron dimeters are referred to as aerosols, and larger liquid particles are usually called droplets. Such procedures are ubiquitous in dental settings when using ultrasonic and sonic scalers, high-speed dental handpieces (tooth preparation with air abrasion, air turbine handpiece), air polishers, and air-water syringes [2, 3]. Despite of some standard control measures (e.g. high volume evacuation, rubber dams) for reducing aerosol generation, these procedures are still the major sources of uncontrolled aerosols and droplets. The major concern with AGPs is that the uncontrolled aerosols and droplets take longer to settle out of the air and/or travel with the airflow to create airborne transmission of respiratory disease.

During the COVID-19 pandemic, one solution to mitigate the risk associated with AGPs is the implementation of an administrative control called fallow time. Following an AGP, a wait-time is undertaken and the operatory is left fallow prior to surface sterilization and the next patient being admitted. The fallow time solution is based on epidemiologic evidence that the vast majority of COVID-19 transmissions occur during close contact with infected individuals, and relies on the assumptions that aerosols and droplets will eventually settle out and be eliminated with surface aseptic techniques and or HVAC integrated filtration. The fallow time technique assumes that the dental operatory is equipped with sufficient air change turnover, so that 90-99% of the air is circulated out and exchanged during the fallow time [4, 5].

Local and Synchronous Control of Covid-19 Airborne Transmission

One major problem with the fallow time solution is that it does not address the infection risk faced by the dentist and assistants during the AGP. Patients or staff in an adjacent dental room may also face the risk unless the rooms are closed and completely isolated, which is difficult from both a physics and pragmatic standpoint; the dental industry has embraced an “open-concept” type operatory, which limits the ability of the fallow time to be effective as potential contaminants are not first physically contained within the confines of the operatory.

Flow physics plays a key role in the airborne dispersion of particles [6]. The understanding of the spread of AGP generated flows inside dental offices during AGPs is limited. Hence, this research focuses on two objectives.

- 1) Study the spread of AGP generated flows inside the dental office during an AGP.
- 2) Investigate a synchronous solution that can control the AGP generated flows from spreading in the dental room.

The synchronous control and removal of the AGP flows can be achieved by a portable extra oral suction device, such as the AIIR device by Care Health Meditech Developments Inc. (www.carehealthmeditech.com) as shown in Fig. 1. The device has a transparent dome placed ~10 to 20 cm above the patient face, and the dome is connected to an electrical negative pressure generator installed in the device cabinet, which creates negative pressure inside the dome to create a local flow sink. The removed AGP flow is filtered and disinfected in the device cabinet, and clean air is discharged back to the room.

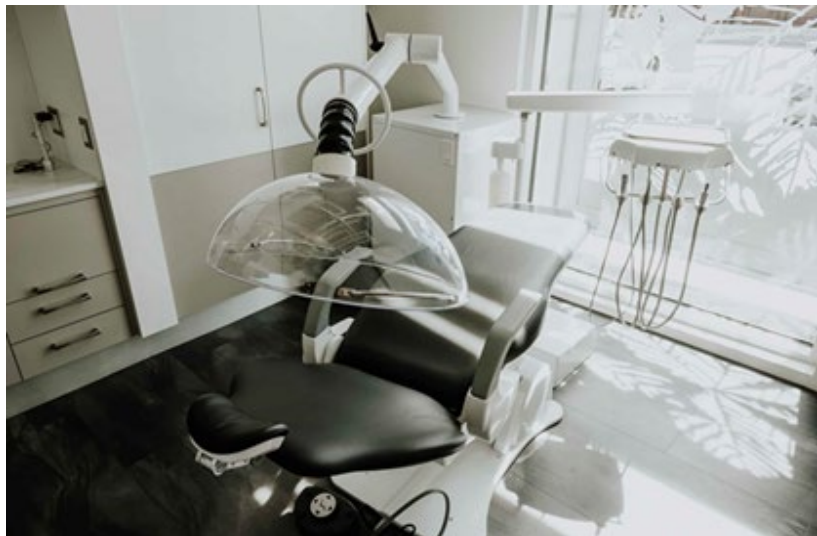


Figure 1: A portable extra oral suction device (AIIR, Care Health Meditech Developments Inc. www.carehealthmeditech.com) for local and synchronous control and removal of AGP flows.

2. Numerical CFD model

The flows exiting the patient mouth during AGP, referred to as AGP flows, includes the patient’s exhalation airflow and the flows generated by dental instruments. AGP flows are multiphase flows, which include air and liquid particles with varied sizes. Particles with very small sizes tend to follow the airflow. For example, if the particle size is much smaller than the mean free path length of room air (~ 70 nm), the particle would behave like a molecule. Large liquid particles interact with airflow with momentum, heat, and mass transport processes. In the present research,

Local and Synchronous Control of Covid-19 Airborne Transmission

numerical simulation is conducted to investigate the flow dynamics of the multiphase flows. The AGP flows are simulated as airflow and dispersed water droplets. The airflow results will help understand the spread of aerosols in real dental settings, and the results of the water droplets will help understand the spread of liquid particles/droplets. Input conditions of the multiphase flows are described in more detail below.

In the numerical model, a dental office is a room with dimensions $10\text{ft} \times 9\text{ft} \times 8\text{ft}$ as shown in Fig. 2. There are two vents on the room ceiling for air change (AC). The airflow through the AC inlet has temperature 22.5°C and relative humidity 50%, and provides 2 ACH (air changes/hour) for the room, which is the standard configuration addressed by commercial building code in most regions.

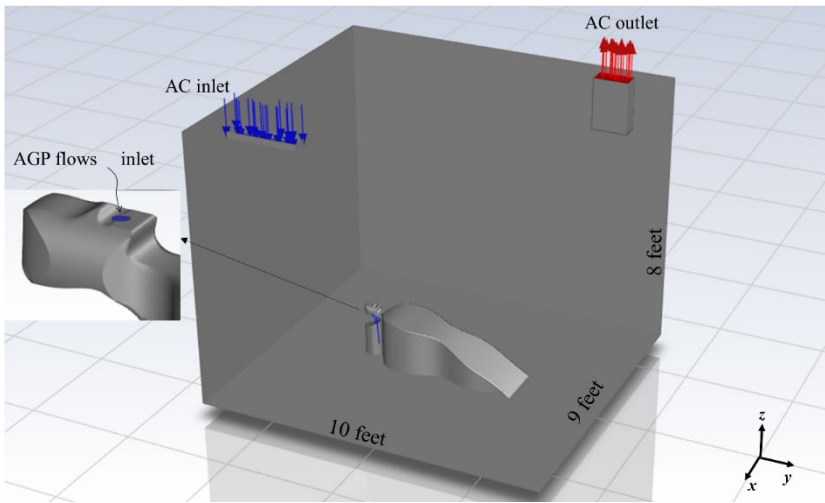


Figure 2: Numerical model of a dental room without synchronous control of AGP flows. (Case- 1).

The AGP flows are introduced at the patient’s mouth as shown in Fig. 2. The AGP airflow is 1 m/s with temperature 36°C and relative humidity 70%, which gives a mass flow rate of $2.278 \times 10^{-2}\text{ kg/min}$. The flow is in the direction 45° from the patient’s chest, i.e. $(u_x, u_y, u_z) = (\sqrt{2}/2, 0, \sqrt{2}/2)\text{ m/s}$. To reflect droplets formed from AGP, three flows of water droplets are released from three injection sources at the patient's mouth, which include two rows of group droplet stream and a surface stream of droplets with varied initial diameters and velocity vectors. The initial conditions of the droplet flows are provided in Table 1.

Table 1: Initial conditions of droplets.

Injection	Injection type	Diameter (μm)	Velocity (u_x, u_y, u_z) (m/s)	Temperature ($^\circ\text{C}$)	Flow rate (kg/min)
1	Group of 50	0.1 to 1000	(1,1,1)	20	3×10^{-7}
2	Group of 50	0.1 to 1000	(1,-1,1)	20	3×10^{-7}
3	Surface	10	(0,0,2)	20	0.6×10^{-7}

Local and Synchronous Control of Covid-19 Airborne Transmission

The model shown in Fig. 2 represents a dental office, where no control measure is taken for AGP flows during the dental procedure. This is numbered as Case-1 in the present work. Another case, numbered Case-2, is shown in Fig. 3, where AIIR is installed in the room. The AIIR device is modeled as two separate pieces. A semi-spherical dome with a constant outlet mass flow rate of 0.065 kg/s and located 12.5 cm above the patient’s face. The AIIR cabinet is included in the model, which has an inlet airflow at a temperature 22.5°C and relative humidity 50%. Its flow rate is the same as the outlet flow rate of the dome. The AC and AGP flows were constant between both cases.

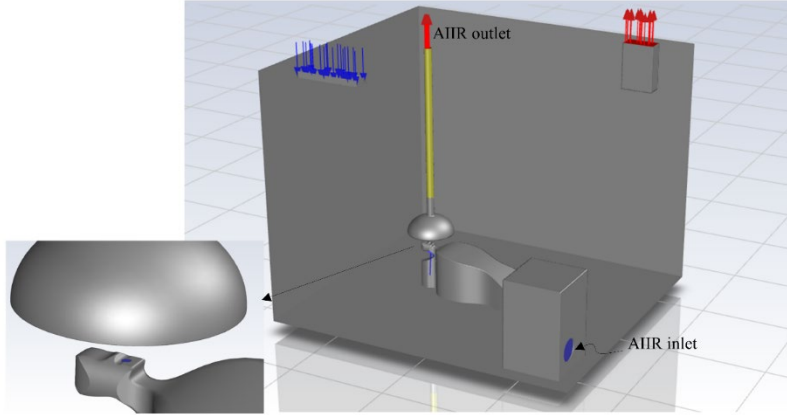


Figure 3: A dental office installed with AIIR to achieve local and synchronous control of AGP flows. (Case-2).

3. CFD governing equations

The flow to be modeled has two phases: a continuous phase and a discrete phase. The continuous phase is the gas flow, which is a binary mixture of air and vapor. Hereinafter, we will still call the continuous phase airflow, and the vapor content in air determines relative humidity. The discrete phase is the droplets emitted from the patient’s mouth. There are multiple flow sources in the room (AC inlet, AGP flows, AIIR discharge) with different temperature and relative humidity, and the vapor pressures are different from the surface of the droplets to the air. As a result, in addition to momentum transfer, the transports of energy and mass also need to be solved.

Simulation is carried out using ANSYS-Fluent [7]. The Euler-Lagrange approach is applied, and the Lagrangian discrete phase model is taken to track the droplets. This methodology is commonly used when interactions between droplets can be neglected. The conservation laws of mass, momentum, and energy are described by the following equations.

The continuity equation for the continuous phase, mixture of air and vapour, is

$$\frac{\partial \rho}{\partial t} + \nabla \cdot (\rho \vec{u}) = S_m \quad (1)$$

Here S_m is a source term, which is the vapor generated from droplet evaporation. Density ρ is the density of the air and vapor mixture, and \vec{u} is the velocity vector.

Local and Synchronous Control of Covid-19 Airborne Transmission

The governing equation for momentum transfer in the continuous phase is

$$\frac{\partial}{\partial t}(\rho \vec{u}) + \nabla \cdot (\rho \vec{u} \vec{u}) = -\nabla p + \nabla \cdot (\bar{\tau}) + \rho \vec{g} + \vec{F} \quad (2)$$

Here p is the static pressure, $\bar{\tau}$ the stress tensor, and \vec{g} the gravitational acceleration. The force per volume \vec{F} is related to the interaction with the droplets. In the present work, the continuous phase is modeled as turbulent flow, for which the standard $k - \varepsilon$ model is used.

The energy conservation for the continuous phase is

$$\frac{\partial}{\partial t}(\rho e) + \nabla \cdot (\vec{u} \rho h) = \nabla \cdot (k \nabla T - \sum_j h_j \vec{j}_j + \bar{\tau} \cdot \vec{u}) + S_h \quad (3)$$

Here h and k are mass-specific enthalpy, and effective thermal conductivity of the air-vapor mixture, respectively. The divergence term on the right hand side includes heat conduction, enthalpy transfer by mass diffusion of air and vapor, and viscous dissipation. The source term S_h is related to the heat and mass transfers with the droplets.

The mass transfer of vapor in the continuous phase is governed by

$$\frac{\partial}{\partial t}(\rho Y_V) + \nabla \cdot (\rho \vec{u} Y_V) = -\nabla \cdot \vec{J}_V + S_m \quad (4)$$

where Y_V is the mass fraction of vapor, and \vec{J}_V is the diffusion flux.

The equation of motion for particles are solved to track the droplet trajectory. Written in a Lagrangian reference frame, the force balance equates the particle inertia with the forces acting on the particle, which is

$$\frac{d(m_d \vec{u}_d)}{dt} = 3\pi d \mu f (\vec{u} - \vec{u}_d) + m_d \frac{\vec{g}(\rho_a - \rho)}{\rho_a} + \vec{a} m_d \quad (5)$$

where m_d , \vec{u}_d , d , ρ_d are the mass, velocity, diameter, and density of the droplets, respectively. Here f is the drag factor, which is the ratio of drag coefficient to the Stokes drag coefficient. The acceleration \vec{a} is associated with the spatiotemporal distribution of \vec{u} .

Considering the droplet as a lumped thermal capacitance, the heat balance equation that relates the particle temperature, $T_d(t)$, to the convective heat transfer and phase change is

$$c_{p,d} m_d \frac{dT_d}{dt} = Nu \frac{k}{d} A_d (T - T_d) + L \frac{dm_d}{dt} \quad (6)$$

where T_d , $c_{p,d}$, A_d are the temperature, specific heat, and area of the droplet. Here Nu is the Nusselt number, and L is the latent heat of vaporization.

The mass transfer due to the vaporization of the droplet follows is governed by

$$\frac{dm_d}{dt} = -Sh \frac{D}{d} A_d \frac{M}{R} \left(\frac{p_{v,d}}{T_d} - RH \frac{p_{sat@T}}{T} \right) \quad (7)$$

Here Sh is the Sherwood number, D the diffusion coefficient of vapor in air, M the molecular weight of vapor, $p_{v,d}$ the vapor pressure at the droplet surface, RH the relative humidity, p_{sat} the saturation vapor pressure.

In the present simulation, the continuous phase is modeled as turbulent flow. To model the turbulent flow, Eq. (2) is time-averaged and becomes the RANS (Reynolds-averaged Navier-Stokes) equation, in which the time derivative disappears. For this steady-state RANS modeling, the $k-\varepsilon$ turbulence model is used [7]. In addition to the equations above, the correlations of f , Nu , and Sh for spherical droplets are required as input to the simulation.

4. Results and discussion

Our discussion in this section will focus on the two-phase flows introduced by the patient's mouth, which simulate the AGP flows in dental procedures. We will track droplet trajectories and observe airflow pathlines, and compare the results of Case-1 (Fig. 2) and Case-2 (Fig. 3).

4.1. Dental office without synchronous control of airborne infection

Simulation is conducted for a dental room without local removal, which is modeled in Fig. 2. Figure 4 shows a few pathlines of the airflow from the patient's mouth, and the color represents the velocity magnitude. The airflow travels around the room with continuous change of velocity directions and magnitudes. All pathlines eventually reach the AC outtake and exit the room. The flow pattern is the result of the thermal-gravitational effect and the interaction with the AC airflow, and the AC airflow is the major factor. Hence, the flow pattern would change for a different AC setting. Nevertheless, Fig. 4 shows room-wide spread and travel of the AGP airflow. In real situations, the airflow is a mixture of air and small aerosol particles. Aerosol particles can easily be carried by the airflow and follow the airflow pathlines as their Stokes numbers are usually small. Brownian diffusion, which is not considered in the model, would also cause aerosol particles to travel between pathlines, thereby resulting in a larger spreading extent.

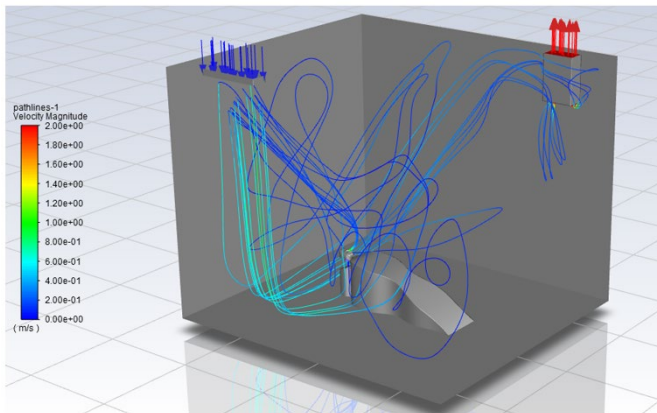


Figure 4: Airflow pathlines of AGP flows in a dental office (Case-1).

The droplets, which are the discrete phase, are traced, and their trajectories are shown in Fig. 5. The momentum of these droplets changes while travelling. This is due to the gravitational force, and drag forces by the airflow. Depending on the initial velocity vector and size, some droplets completely evaporate in flight. This is visible from the upward trajectory lines which terminate in the air. Some droplets fall on surfaces (floor, chair, patient, etc.) before complete evaporation. Due to using pure water droplets, the evaporation rate here can be considered as overestimated versus a real-life situation, e.g. droplets of saliva. Additionally, droplets may not completely evaporate if they contain particles. The evaporation reduces the droplet to the size range of aerosol particles. So it is reasonable to say that the droplets that disappeared in flight in Fig. 5 become aerosol

Local and Synchronous Control of Covid-19 Airborne Transmission

particles. These small particles would continue their travel inside the room by following the pathline which overlaps with the ending part of their early trajectory.

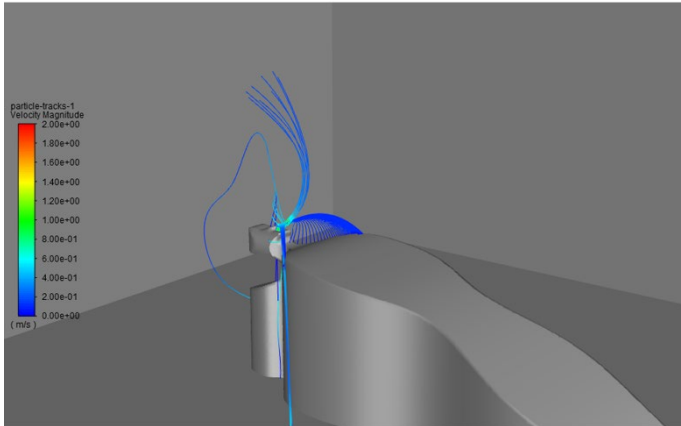


Figure 5: Droplet traces colored by velocity magnitude (Case-1).

Figures 4 & 5 show the travel paths of airflow and droplets. It is also important to know for how long aerosol particles and droplets can be travelling in the room. The time length taken for a fluid particle to travel from one location, say its starting point in the numerical domain, to another location on its pathline can be calculated using

$$\tau = \int_0^\tau dt = \int_0^l \frac{1}{u} ds \tag{8}$$

Here l is the distance along the pathline from the starting point to the location in question, and u is the local velocity along the pathline, dt is a differential time, and ds is a differential travel distance.

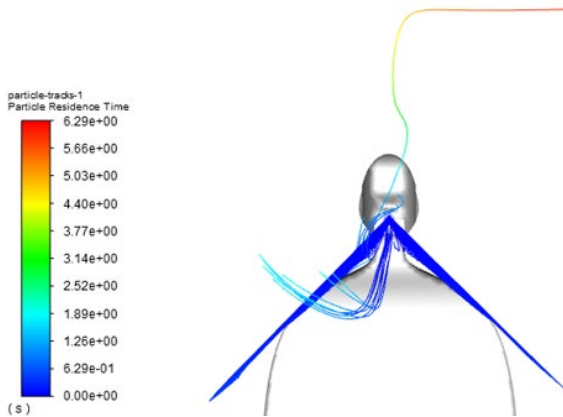


Figure 6: Droplet traces colored by droplet residence time. (Case-1).

Using Eq. (8) along with the results presented in Fig. 4, we obtain the residence time for droplets before they either completely evaporate or land on surfaces. The results are shown in Fig. 6, where

Local and Synchronous Control of Covid-19 Airborne Transmission

the local color on each trajectory curve indicates how long is taken for the droplet to reach that location. It can be seen that the droplets can exist in air for a few seconds only. Based on the velocity data shown in Fig. 5, we apply Eq. (8) to obtain pathline time, which is shown with color scale in Fig. 7. Within the tracked pathlines, the maximum pathline time is 328 seconds. This means a small aerosol particle can be travelling in the room for more than 5 minutes. It should be noted that this time length could be significantly underestimated as the Brownian diffusion of aerosol particles are not included in the model.

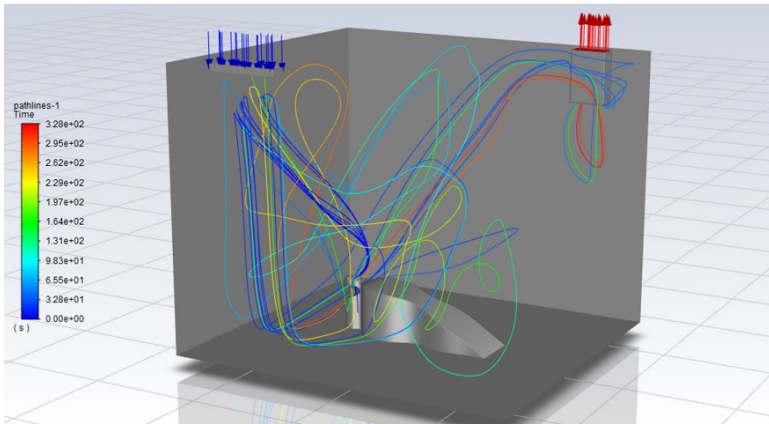


Figure 7: Pathline time for AGP airflow. (Case-1).

4.2. Dental office installed with AIIR

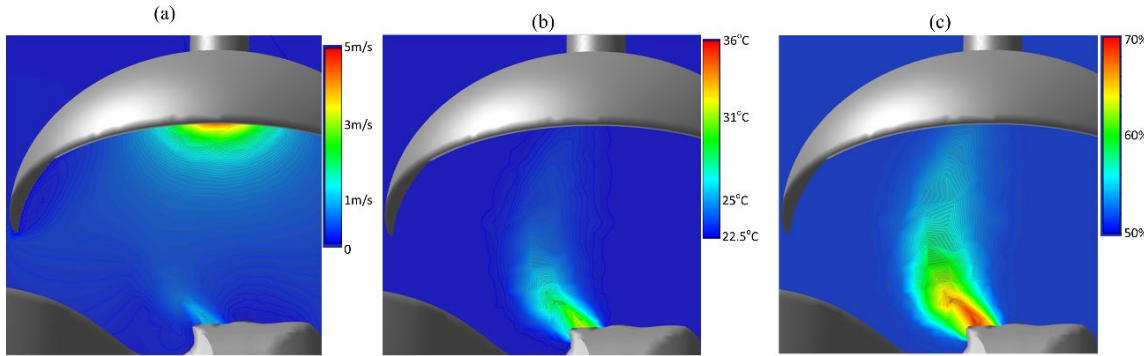


Figure 8: Airflow in the region between the patient and the AIIR dome: (a) velocity; (b) temperature; (c) relative humidity. (Case-2)

The model for a dental office installed with AIIR to implement synchronous control of AGP flows has been shown in Fig. 3. Simply speaking, the dome-shaped collector of AIIR serves as a local flow sink. This can be seen from Fig. 8, which shows the distributions velocity, temperature, and relative humidity in the region between the patient and the dome. Figure 8a shows how the existence of the dome affects the airflow velocity. Close to the patient’s mouth, the velocity is ~ 1 m/s, which is the input velocity of the AGP airflow. Inside the dome, velocity increases as the flow area decreases. Figure 8b shows the temperature distribution. It indicates the heat exchange

Local and Synchronous Control of Covid-19 Airborne Transmission

between the AGP flows and the AC flow when the AGP flows are moving toward the dome. Figure 8c shows the mass transfer of vapor from the AGP flows to the AC flow, and the distribution of relative humidity indicates the flow motion of the AGP flows.

Next, we discuss the continuous phase of the AGP flows. Figure 9 shows a few pathlines of the airflow originated from the AGP. From Fig. 9a, we can clearly see that the AGP airflow does not spread to the room due to the local and synchronous control. A close-up view is shown in Fig. 9b, which shows all the pathlines enter the AIIR suction tube, and the velocity accelerates to more than 20 m/s. Figure 9c shows the same pathlines with color indicating the pathline time. For a small aerosol particle, it would take less than one second for the particle to be removed by the AIIR device.

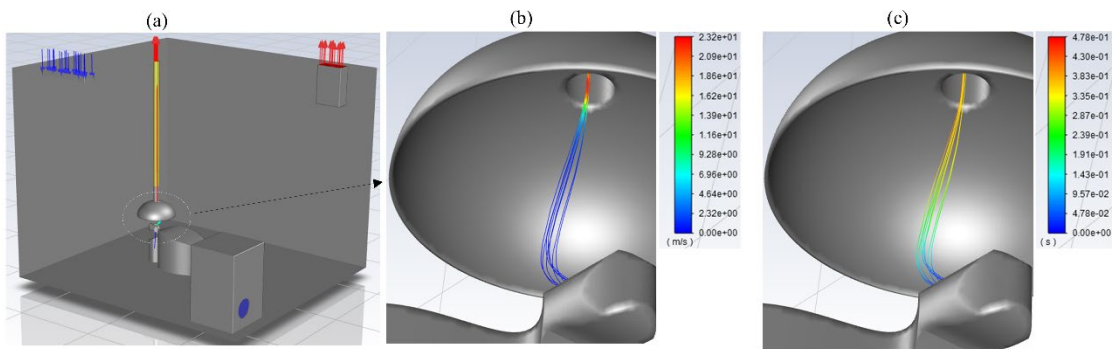


Figure 9: AGP airflow in the dental office installed with AIIR (Case-2).

The results of the droplets are shown in Fig. 10. Figure 10a shows the trajectories of the input droplets, and the color is related to the droplet size. It is expected to see in Fig. 10a that large droplets fall on surfaces due to the domination of gravitational force. Figure 10b shows that small droplets are accelerated by the suction flow inside the dome. Figure 10c shows the trajectory times of the droplets. It takes less than 1 second to remove the small droplets. For large droplets, it takes a few seconds to land on surfaces. No droplets were observed to spread together with the airflow inside the room.

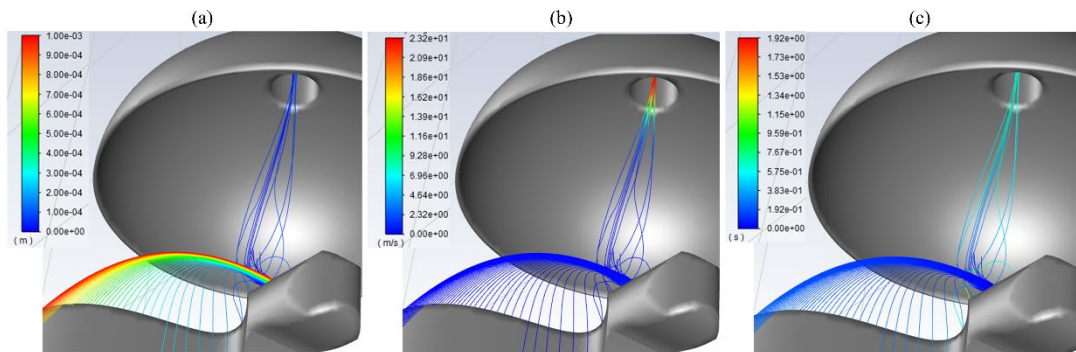


Figure 10: Traces of droplets in a dental office installed with AIIR (Case-2).

5. Conclusions

Dental AGPs can emit aerosols and droplets, which together with air form two-phase flows. CFD simulation was conducted to investigate the momentum, heat, and mass transfers of the two-phase flows interacting with air change flow in model dental offices. Two numerical models are considered: a dental office without any extra control of AGP flows during the dental procedure; and a dental office installed with AIIR to achieve local and synchronous control of AGP flows.

The results show significant spatial and temporal differences between the two cases. The spatial difference can be described as follows. During the dental procedure droplets and aerosols are expected to spread widely inside the dental office if no control measure is taken, which would put people inside the dental room and other rooms at potential infection risk. Results also show that using AIIR device synchronous and local control can be achieved, which isolate the AGP flows from spreading and travelling in the dental room. The temporal difference between the two cases can be summarized by Table 2.

Table 2: Comparison between a dental office without local and synchronous control of AGP flows and a dental office installed with AIIR.

	Dental office without AGP control	Dental office installed with AIIR
Droplets residence time	6 s	2 s
Airflow pathline time (aerosol)	328 s	< 1 s

In conclusion, this CFD simulation research indicates that a local and synchronous engineering control, such as using a portable extra oral suction device, appears to be an effective mitigation strategy to reduce potential infection risks created by AGP in a dental office. The local and synchronous engineering control provides the advantage of

- a) More quickly removing aerosols and droplets,
- b) Preventing aerosols and droplets from circulating widely in the operatory,
- c) Providing better airborne infection protection potential to other patients in the practice and dental care workers.

Notes to Open Synchronous Devices / Air Purifiers

It is noted that many commercial settings have opted to include extra air circulation devices, commonly referred to as “air purifiers” or “air scrubbers” in an effort to reduce fallow times and / or negate the requirement for closed operatory. These devices are usually placed in the room corner, and can only take room air with already dispersed particles. As such, it is recommended that at source, local and synchronous collection devices be considered ahead of this type of solution.



6. References

- [1] Worldometers.info, COVID-19 CORONAVIRUS PANDEMIC, October 28, 2020, 17:55 GMT, <https://www.worldometers.info/coronavirus/>.
- [2] Harrel SK, Molinari J. Aerosols and splatter in dentistry. A brief review of the literature and infection control implications. *The Journal of the American Dental Association* 2004, 135, 429-437.
- [3] Raghunath N, Meenakshi S, Sreeshyla HS, Priyanka N. Aerosols in dental practice-A neglected infectious vector. *Microbiology Research Journal International* 2016; 15:1-8.
- [4] Ontario Agency for Health Protection and Promotion (Public Health Ontario). COVID-19 in dental care settings. Toronto, ON: Queen's Printer for Ontario; 2020.
- [5] CSA Group. CSA Z317.2:19: Special requirements for heating, ventilation, and air-conditioning (HVAC) systems in health care facilities. Toronto, ON: CSA Group; 2019.
- [6] Mittal, Rajat, Rui Ni, and Jung-Hee Seo. "The flow physics of COVID-19." *Journal of fluid Mechanics* 894 (2020).
- [7] ANSYS Fluent Theory Guide, ANSYS Inc. 2020.